

# Two-Loop Electroweak Corrections for the $K \rightarrow \pi\nu\bar{\nu}$ Decays

Joachim Brod<sup>a,b</sup>, Martin Gorbahn<sup>a,b</sup>, and Emmanuel Stamou<sup>a,b,c</sup>

<sup>a</sup>Excellence Cluster Universe, Technische Universität München,  
Boltzmannstraße 2, D-85748 Garching, Germany

<sup>b</sup>Institute for Advanced Study, Technische Universität München,  
Lichtenbergstraße 2a, D-85748 Garching, Germany

<sup>c</sup>Physik-Department, Technische Universität München,  
James-Franck-Straße, D-85748 Garching, Germany

September 2010

## Abstract

The rare  $K \rightarrow \pi\nu\bar{\nu}$  decays play a central role in testing the Standard Model and its extensions. Upcoming experiments plan to measure the decay rates with high accuracy. Yet, unknown higher-order electroweak corrections result in a sizeable theory error. We remove this uncertainty by computing the full two-loop electroweak corrections to the top-quark contribution  $X_t$  to the rare decays  $K_L \rightarrow \pi^0\nu\bar{\nu}$ ,  $K^+ \rightarrow \pi^+\nu\bar{\nu}$ , and  $B \rightarrow X_{d,s}\nu\bar{\nu}$  in the Standard Model. The remaining theoretical uncertainty related to electroweak effects is now far below 1%. Finally we update the branching ratios to find  $\text{Br}(K_L \rightarrow \pi^0\nu\bar{\nu}) = 2.43(39)(6) \times 10^{-11}$  and  $\text{Br}(K^+ \rightarrow \pi^+\nu\bar{\nu}) = 7.81(75)(29) \times 10^{-11}$ . The first error summarises the parametric, the second the remaining theoretical uncertainties.

## 1 Introduction

The branching ratios of the rare  $K^+ \rightarrow \pi^+\nu\bar{\nu}$  and  $K_L \rightarrow \pi^0\nu\bar{\nu}$  decays are dominated by contributions of internal top-quarks in the Standard Model. This short distance sensitivity results in a precise theory prediction, but also in a proportionality to powers of  $V_{ts}^*V_{td}$ . Accordingly, the branching ratios are suppressed with respect to generic new physics scenarios by the near diagonality of the Cabibbo-Kobayashi-Maskawa (CKM) matrix. This

leads to a high sensitivity to new physics, and a precision measurement of these modes could provide a decisive test of the Standard Model and its extensions.

This potential will be exploited by a new generation of experiments (NA62 at CERN, KOTO at JPARC, and the proposed future experiment P996 at Fermilab), which aim at measuring the branching ratios with unprecedented precision.

In the Standard Model the  $K \rightarrow \pi\nu\bar{\nu}$  decays proceed through  $Z$ -penguin and electroweak box diagrams which exhibit a power-like GIM mechanism. This implies a suppression of non-perturbative effects and, related to this, that the low-energy effective Hamiltonian [1, 2]

$$\mathcal{H}_{\text{eff}} = \frac{4G_F}{\sqrt{2}} \frac{\alpha}{2\pi \sin^2 \theta_W} \sum_{l=e,\mu,\tau} (\lambda_c X^l + \lambda_t X_t) (\bar{s}_L \gamma_\mu d_L) (\bar{\nu}_{lL} \gamma^\mu \nu_{lL}) + \text{h.c.} \quad (1.1)$$

involves to an excellent approximation only a single effective operator. Here  $G_F$  is the Fermi constant,  $\alpha$  the electromagnetic coupling and  $\theta_W$  the weak mixing angle. The sum is over all lepton flavours,  $\lambda_i = V_{is}^* V_{id}$  comprise the CKM factors, and  $f_L$  represents left-handed fermion fields.

The functions  $X^l$  constitute the charm-quark contribution to  $\mathcal{H}_{\text{eff}}$  and add 30% to the total branching ratio of the  $K^+ \rightarrow \pi^+ \nu \bar{\nu}$  decay, while they leave the CP violating  $K_L \rightarrow \pi^0 \nu \bar{\nu}$  decay unaffected. The theoretical uncertainty in  $X^l$  is 2.5% after next-to-next-to-leading order (NNLO) QCD [3, 4, 5] and next-to-leading order (NLO) electroweak corrections [6] are taken into account, and the resulting error in the branching ratio is small.

The situation is different for the function  $X_t$  which includes internal top-quark loops: it gives either the sole or the dominant contribution to the neutral or the charged decay modes, respectively. A two-loop electroweak calculation should cancel the sizeable scheme dependence of the input parameters. Yet, only NLO QCD corrections [2, 7, 8] and the leading term of the large- $m_t$  expansion of the two-loop electroweak corrections are known. While unknown higher-order QCD corrections result in a 1% uncertainty in  $X_t$ , the uncertainty related to unknown sub-leading electroweak contributions is estimated to be  $\pm 2\%$  [9]. This can be understood in the following way: the matching calculation with internal top-quark loops is purely short distance, the resulting operator renormalises like a current, such that the QCD perturbation theory converges well. Yet the on-shell scheme counterterm of  $\sin \theta_W$  includes large higher terms in the large- $m_t$  expansion. Hence the renormalisation scheme dependence of  $\alpha/\sin^2 \theta_W$  in (1.1) cannot cancel if only the leading term in the large- $m_t$  expansion is taken into account. This was found in Reference [9] where the scheme difference between the on-shell scheme and the  $\overline{\text{MS}}$  scheme was only decreased from 5.6% to 3.4% through the inclusion of the first order in the large- $m_t$  expansion.

In this paper we will improve on the analysis of Reference [9] and compute the full electroweak two-loop corrections to the top-quark contribution  $X_t$ . Only in such a way is it possible to fix the definition of the electroweak input parameters and reduce the uncertainty due to unknown higher order electroweak corrections from 2% to the per mil level. Since a 2% uncertainty in  $X_t$  scales up to a 3% to 4% uncertainty in the branching

ratios such a reduction of the theoretical error is important in particular in light of the coming experiments. In addition, our results are equally applicable for the  $B \rightarrow X_{d,s}\nu\bar{\nu}$  decays.

Our paper is organised as follows. In Section 2 we discuss the dependence of our result on different renormalisation schemes. In Section 3 we present some technical details of our calculation. Our numerical results are contained in Section 4. In the Appendices we provide the analytic form of the electroweak correction to  $X_t$  in the limit of small  $\sin\theta_W$  and compare our expansion for a large top-quark mass with the literature.

## 2 $X_t$ beyond leading order

The truncation of the perturbation theory results in a residual scale and scheme dependence of the matrix elements of the effective Hamiltonian in Equation (1.1). For the top-quark contribution, the matrix element of the operator

$$Q_\nu = \sum_{l=e,\mu,\tau} (\bar{s}_L\gamma_\mu d_L)(\bar{\nu}_{lL}\gamma^\mu\nu_{lL}) \quad (2.1)$$

factorises and  $4\alpha G_F/(2\sqrt{2}\pi\sin^2\theta_W)\lambda_t X_t$  will be independent of the renormalisation procedure after higher-order corrections are included. Let us now discuss the dependence on the electroweak renormalisation scheme and how to combine these schemes with the NLO QCD results, which are known in the  $\overline{\text{MS}}$  scheme.

Pure QCD corrections leave  $G_F$ ,  $\alpha$ , and  $\sin^2\theta_W$  unaffected, such that  $X_t$  is a renormalisation scheme invariant quantity if electroweak effects are ignored. It is then customary to expand

$$X_t = X_t^{(0)} + \frac{\alpha_s}{4\pi} X_t^{(1)} + \frac{\alpha}{4\pi} X_t^{(EW)}. \quad (2.2)$$

in terms of the leading-order (LO) contribution [10]

$$X_t^{(0)} = \frac{x_t}{8} \left[ \frac{x_t + 2}{x_t - 1} + \frac{3x_t - 6}{(x_t - 1)^2} \ln x_t \right], \quad (2.3)$$

where  $x_t = m_t^2/M_W^2$ . The schemes for  $m_t$  and  $M_W$  are defined below. The NLO QCD correction [2, 7, 8]

$$\begin{aligned} X_t^{(1)} = & -\frac{29x_t - x_t^2 - 4x_t^3}{3(1-x_t)^2} - \frac{x_t + 9x_t^2 - x_t^3 - x_t^4}{(1-x_t)^3} \ln x_t \\ & + \frac{8x_t + 4x_t^2 + x_t^3 - x_t^4}{2(1-x_t)^3} \ln^2 x_t - \frac{4x_t - x_t^3}{(1-x_t)^2} \text{Li}_2(1-x_t) + 8x_t \frac{\partial X_t^{(0)}}{\partial x_t} \ln \frac{\mu_t^2}{M_W^2}, \end{aligned} \quad (2.4)$$

fixes the renormalisation scheme of the parameters which appear in the LO contribution: namely, the top-quark mass. Here, the QCD part of the top-quark mass counterterm is defined in the  $\overline{\text{MS}}$  scheme.

The leading term in the large- $m_t$  expansion of the two-loop electroweak corrections  $X_t^{(EW)}$  can be found in Reference [9], while the hitherto unknown full two-loop result is computed in this paper. The sum of  $X_t^{(0)}$  and  $X_t^{(EW)}$  will only be invariant under an electroweak scheme change if it is multiplied by the normalisation factor of the effective Hamiltonian,  $4\alpha G_F/(2\sqrt{2}\pi \sin^2 \theta_W)$ . Accordingly, the electroweak renormalisation scheme has to be fixed for the parameters in the normalisation factor.

Since in the electroweak theory not all parameters are independent, we have to specify the physical input parameters, and we choose the set

$$G_F, \alpha, M_Z, M_t, \text{ and } M_H. \quad (2.5)$$

Here  $G_F$  is the experimental value of the Wilson coefficient relevant for muon decay,  $\alpha$  the fine structure constant, and  $M_Z$  the  $Z$ -boson pole mass.  $M_t$  is the top-quark mass, where QCD corrections are renormalised in the  $\overline{\text{MS}}$  scheme, while the on-shell scheme is used for the electroweak corrections. The Higgs mass  $M_H$  is essentially a free parameter – its value is assumed to be consistent with electroweak precision data.

For fixed input parameters we can now study the remaining residual higher-order uncertainty by using different renormalisation schemes. In the following discussion we will make use of three renormalisation schemes:

- The  $\overline{\text{MS}}$  scheme for all parameters,
- the on-shell scheme for all masses and the  $\overline{\text{MS}}$  scheme for all coupling constants,
- or the on-shell scheme for all masses and the weak mixing angle – the QED coupling constant is renormalised in the  $\overline{\text{MS}}$  scheme.

The explicit result for  $X_t^{(EW)}$  is different for each renormalisation scheme. In practise, we perform our calculation in the  $\overline{\text{MS}}$  scheme and transform our result into the respective scheme by a finite renormalisation.

In all three schemes we renormalise the CKM parameters in the  $\overline{\text{MS}}$  scheme and use  $G_F$  as a normalisation factor for the effective Hamiltonian in Equation (1.1). The parameter  $G_F$  plays a special role, because it is by itself defined as a Wilson coefficient, of the operator  $Q_\mu = (\bar{\nu}_{\mu L} \gamma_\rho \mu_L)(\bar{e}_L \gamma^\rho \nu_{eL})$  which induces the muon decay in the effective Fermi theory. To make this more explicit we introduce the following notation: We denote the Wilson coefficient for muon decay by  $G_\mu = G_\mu^{(0)} + G_\mu^{(EW)} + \dots$ , where the superscript (0) denotes the tree level contribution, (EW) the one-loop electroweak corrections, and the ellipses stand for terms beyond second order in the electroweak interactions. By  $G_F$  we then denote the experimental value of  $G_\mu$  as extracted from muon life-time experiments [11, 12]. If we now write the effective Hamiltonian (1.1) in the general form

$$\mathcal{H}_{\text{eff}} = \frac{4}{\sqrt{2}} \frac{\alpha}{2\pi \sin^2 \theta_W} C_\nu Q_\nu = \frac{4G_F}{\sqrt{2}} \frac{\alpha}{2\pi \sin^2 \theta_W} X_t Q_\nu, \quad (2.6)$$

we find

$$X_t^{(0)} = \frac{C^{(0)}}{G_\mu^{(0)}}, \quad X_t^{(EW)} = \frac{C^{(EW)}}{G_\mu^{(0)}} - \frac{C^{(0)} G_\mu^{(EW)}}{(G_\mu^{(0)})^2}. \quad (2.7)$$

## The $\overline{\text{MS}}$ Scheme

In the  $\overline{\text{MS}}$  scheme we use

$$g_1, g_2, v, \lambda, \text{ and } y_t \tag{2.8}$$

as fundamental parameters. Here  $g_1$  and  $g_2$  are the couplings of the  $SU(2)$  and  $U(1)$  gauge group, respectively,  $v$  is the vacuum expectation value of the Higgs field,  $\lambda$  the quartic Higgs self coupling, and  $y_t$  the Yukawa coupling of the top quark. All these parameters are running parameters, depending on the renormalisation scale  $\mu$ . We fix the initial conditions of these parameters by expressing the physical parameter set (2.5) through (2.8) using one-loop accuracy<sup>1</sup> and fitting the values of (2.8) to yield the experimental values of (2.5).

We choose to cancel all tadpole diagrams with a finite counterterm. This results in an additional finite renormalisation of all massive quantities – a sample diagram is shown in Figure 1. In this way we ensure that intermediate results are gauge parameter independent.

## Masses in the On-Shell Scheme

As a more well-behaved alternative, we use the on-shell definition of the  $W$ -boson and the top-quark mass. Since we performed our calculation in the  $\overline{\text{MS}}$  scheme, we have to perform a finite mass renormalisation. The necessary renormalisation constants consistent with our treatment of tadpole diagrams can be found in [13, 14].

In addition, we have to specify the renormalisation scheme for the weak mixing angle. We will use the following two schemes:

- In the on-shell scheme the weak mixing angle is defined by  $s_W^2 \equiv \sin^2 \theta_W^{\text{on-shell}} = 1 - M_W^2/M_Z^2$ . Here the  $W$ -boson mass is calculated including radiative corrections from the input parameter set (2.5), which introduces a Higgs-mass dependence. In addition, the use of the on-shell value for  $\sin^2 \theta_W$  implies a finite renormalisation of our  $\overline{\text{MS}}$  results by including a finite counterterm for  $\sin^2 \theta_W$ . It is given in terms of the on-shell renormalisation constants for  $M_W$  and  $M_Z$  by

$$\delta s_W = \frac{c_W^2}{2s_W} \left( \frac{\delta M_Z^2}{M_Z^2} - \frac{\delta M_W^2}{M_W^2} \right) \Big|_{\Delta=0}, \tag{2.9}$$

where the subscript  $\Delta = 0$  implies setting the pole part including the finite subtraction,  $\Delta = 1/\epsilon - \gamma_E + \log 4\pi$ , to zero. The expressions for  $\delta M_Z^2$  and  $\delta M_W^2$  can again be found in [13, 14].

- The  $\overline{\text{MS}}$  definition of the weak mixing angle, denoted by  $\hat{s}_{\text{ND}}$ , leads to numerically tiny NLO corrections. It is given in terms of  $s_W^2$  by [15]

$$\hat{s}_{\text{ND}}^2 \equiv \sin^2 \theta_W^{\overline{\text{MS}}} = s_W^2 \left( 1 + \frac{c_W^2}{s_W^2} \frac{4\pi \hat{\alpha}(M_Z)}{\hat{s}_{\text{ND}}^2} \Delta \hat{\rho} \right), \tag{2.10}$$

---

<sup>1</sup>For the Higgs boson mass we use the tree-level relation.

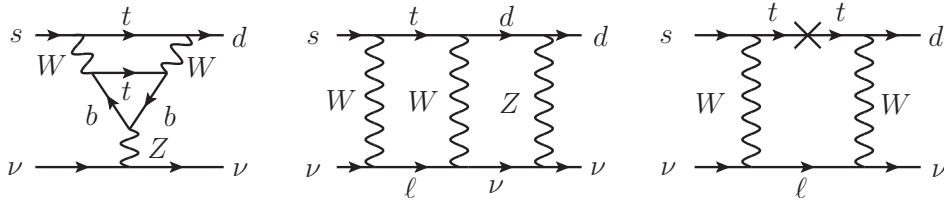


Figure 1: Sample penguin, box, and counterterm diagrams. Our tadpole renormalisation results in an explicit finite renormalisation of all massive quantities. The right-hand side diagram shows a resulting counterterm diagram.

where  $\hat{\alpha} = \alpha^{\overline{\text{MS}}}$ , and  $c_W^2 = 1 - s_W^2$ . The explicit expression for  $\Delta\hat{\rho}$  can also be found in [15].

The numerical discussion of the three different schemes is given in Section 4.

### 3 Calculation

We determine the effective Hamiltonian by computing the relevant Standard Model Green's functions in the  $\overline{\text{MS}}$  scheme and matching them to the five-flavour effective theory. To this end we have to calculate two-loop box and penguin diagrams, samples of which are shown in Figure 1. All diagrams reduce to two-loop vacuum diagrams after setting external momenta and light masses to zero. The resulting loop integrals are computed using standard methods [16, 17]. All this is done in two independent setups: one is using the FeynArts [18] package to generate the diagrams and a self written Mathematica program, the other method uses a self written Form [19] program. The Feynman gauge  $\xi = 1$  is used in both setups.

The integrals in the effective theory correspond to massless diagrams with vanishing external momenta and are exactly zero in dimensional regularisation. The only remaining contributions are then products of renormalisation constants and tree-level matrix elements of the operators  $Q_\nu$ , defined in Equation (2.1), and

$$E_\nu = \sum_{l=e,\mu,\tau} (\bar{s}_L \gamma_{\mu_1} \gamma_{\mu_2} \gamma_{\mu_3} d_L) (\bar{\nu}_{lL} \gamma^{\mu_1} \gamma^{\mu_2} \gamma^{\mu_3} \nu_{lL}) - (16 - 4\epsilon) Q_\nu. \quad (3.1)$$

The evanescent operator  $E_\nu$  arises in the context of dimensional regularisation and vanishes algebraically in four space-time dimensions. It leads to a non-vanishing finite contribution to the Wilson coefficient, proportional to the finite mixing of  $E_\nu$  into  $Q_\nu$ . The infinite operator renormalisation constants are determined from the ultraviolet poles of the matrix elements of the operators between external fermion states. They multiply the tree-level and one-loop Wilson coefficients of the operators (2.1) and (3.1) and cancel exactly the corresponding spurious infrared divergences of the Standard Model amplitude, thus rendering the matching condition finite.

The use of dimensional regularisation is in general inconsistent with a fully anticommuting  $\gamma_5$  matrix in  $d$  dimensions, and we use the 't Hooft-Veltman (HV) scheme in our

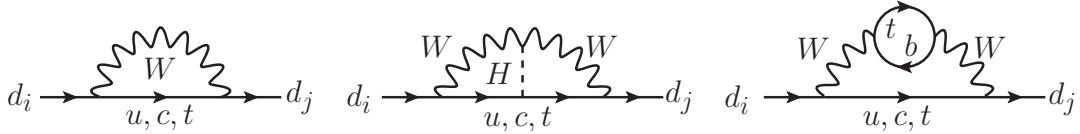


Figure 2: Sample diagrams which imply an off-diagonal field renormalisation.

calculation. However, problems only arise when computing traces containing at least three  $\gamma_5$  matrices, appearing in the anomalous fermion triangles (see for instance the first diagram in Figure 1). In all other cases we can use a naive anticommuting  $\gamma_5$  (NDR scheme), which avoids spurious finite renormalisations required in the HV scheme [20].

We have performed our calculation in the  $\overline{\text{MS}}$  scheme as described in Section 2. The renormalisation of masses and couplings is performed in the usual way.

In order to ensure the canonical form of the kinetic term for the down-type quarks,  $i\bar{d}_{L,k}\not{D}d_{L,j}$ , in the effective theory, we perform a finite off-diagonal field renormalisation. The exchange of  $W$  bosons induces transitions between quarks of different generations (cf. Figure 2). We rediagonalise the kinetic term by including a suitable finite part in the (matrix-) field renormalisation  $Z_{L,ij}^{1/2}$ :

$$d_{L,i}^{\text{bare}} = Z_{L,ij}^{1/2} d_{L,j}, \quad (3.2)$$

where  $i$  denotes the generation of the down-type fermion ( $i = 1, 2, 3$ ).

The renormalisation leads to a finite result for  $X_t^{(EW)}$ . As an additional check we also verified that the full result is analytically independent of the renormalisation scale  $\mu$ .

## 4 Numerics

In this section we present our numerical results and discuss the theoretical uncertainty of the branching ratios of the rare Kaon decays. For our numerical analysis we use the central values and errors of the input parameters given in Table 1. As discussed in detail in Section 2, we use  $\alpha$ ,  $G_F$ , and  $M_Z$  as the basic input parameters for the electroweak theory. The mass of the  $W$  boson is then not an independent quantity; we calculate its mass using the approximate formula given in Reference [21], which includes the state-of-the-art higher order corrections.

Converting the on-shell top-quark mass  $M_t^{\text{TEV}}$ , measured at Tevatron, to the  $\overline{\text{MS}}$  scheme using three-loop QCD accuracy, we find  $M_t \equiv m_t^{\overline{\text{MS}},\text{QCD}}(m_t) = 163.7 \text{ GeV}$ . For this conversion as well as for the QCD running of  $M_t$  and  $\alpha_s$  we use the Mathematica package RunDec [22].

The electroweak correction term  $X_t^{(EW)}$  cancels the scheme and scale dependence of the prefactor  $\alpha/\sin^2\theta_W$  up to higher orders in the electroweak interaction. The remaining scheme and scale dependence will serve as an estimate of the theoretical uncertainty of our

Parameter	Value	Ref.	Parameter	Value	Ref.
$M_Z$	91.1876(21) GeV	[23]	$\alpha_s(M_Z)$	0.1184(7)	[23]
$M_H$	155(40) GeV		$\hat{\alpha}^{-1}(M_Z)$	127.925(16)	[23]
$M_t^{\text{TEV}}$	173.3(1.1) GeV	[24]	$G_F$	$1.166\,367(5) \times 10^{-5} \text{ GeV}^{-2}$	[23]
$m_c(m_c)$	1.279(13) GeV	[25]	$\lambda$	0.2255(7)	[26]
$\hat{s}_{\text{ND}}^2(M_Z)$	0.2315(13)	[23]	$ V_{cb} $	$4.06(13) \times 10^{-2}$	[23]
$\kappa_+$	$0.5173(25) \times 10^{-10}$	[27]	$\bar{\rho}$	$0.141_{-0.017}^{+0.029}$	[28]
$\kappa_L$	$2.231(13) \times 10^{-10}$	[27]	$\bar{\eta}$	0.343(16)	[28]
$ \epsilon_K $	$2.228(11) \times 10^{-3}$	[23]			

Table 1: Input parameters used in our numerical analysis.

result. To facilitate the discussion, we define the scale and scheme independent quantity

$$\tilde{X}_t = \frac{\alpha(\mu, M_H)}{\alpha(\mu = M_Z, M_H = 155 \text{ GeV})} \frac{\sin^2 \theta_W(\mu = M_Z, M_H = 155 \text{ GeV})}{\sin^2 \theta_W(\mu, M_H)} X_t(\mu). \quad (4.1)$$

It is formally independent of  $\mu$  and coincides with  $X_t(\mu)$  at  $\mu = M_Z$  and  $M_H = 155 \text{ GeV}$ . We normalise  $\tilde{X}_t$  to our central value for the Higgs-boson mass,  $M_H = 155 \text{ GeV}$ ; as we will see below, the dependence on  $M_H$  is very weak for  $115 \text{ GeV} < M_H < 200 \text{ GeV}$ . The function  $\tilde{X}_t$  is plotted in Figure 3 for  $M_H = 155 \text{ GeV}$ . Here the dashed line shows the LO result. As is clearly visible, the inclusion of the two-loop electroweak corrections (solid line) cancels the scale dependence of the electroweak input parameters almost completely, up to negligible corrections of 0.02%.

Next we discuss the dependence of our result on the choice of the renormalisation scheme. The difference between the  $\overline{\text{MS}}$  and on-shell definition of the parameters  $\sin^2 \theta_W$  and  $m_t^2$ , appearing in the LO effective Hamiltonian, amounts to roughly 4% and 7%, respectively, leading to a large dependence of the branching ratios on the renormalisation scheme, if the two-loop electroweak corrections are not included. In turn, we will see that the inclusion of  $X_t^{(EW)}$  cancels this ambiguity almost completely. To get a quantitative estimate, we evaluate the function  $X_t$  numerically in the three renormalisation schemes described in Section 2.

In Figure 4 we show  $\tilde{X}_t$  in dependence on the Higgs boson mass  $M_H$ , where all couplings are defined in the  $\overline{\text{MS}}$  scheme and all masses in the on-shell scheme. In this scheme the NLO electroweak corrections are tiny, of the order of one per mil, even for very large Higgs masses.

In Figure 5 we compare the results in two other schemes. In the left panel we show  $\tilde{X}_t$ , where all parameters are defined in the  $\overline{\text{MS}}$  scheme. In the right panel, all parameters are defined in the on-shell scheme, apart from  $\alpha$ , which is defined in the  $\overline{\text{MS}}$  scheme. As expected, we observe that for the on-shell definition of  $\sin^2 \theta_W$  (right panel) the related ambiguity is cancelled by a sizeable ( $\approx 4\%$ ) two-loop correction, whereas for the full  $\overline{\text{MS}}$  definition (left panel) the electroweak corrections amount to 1%.

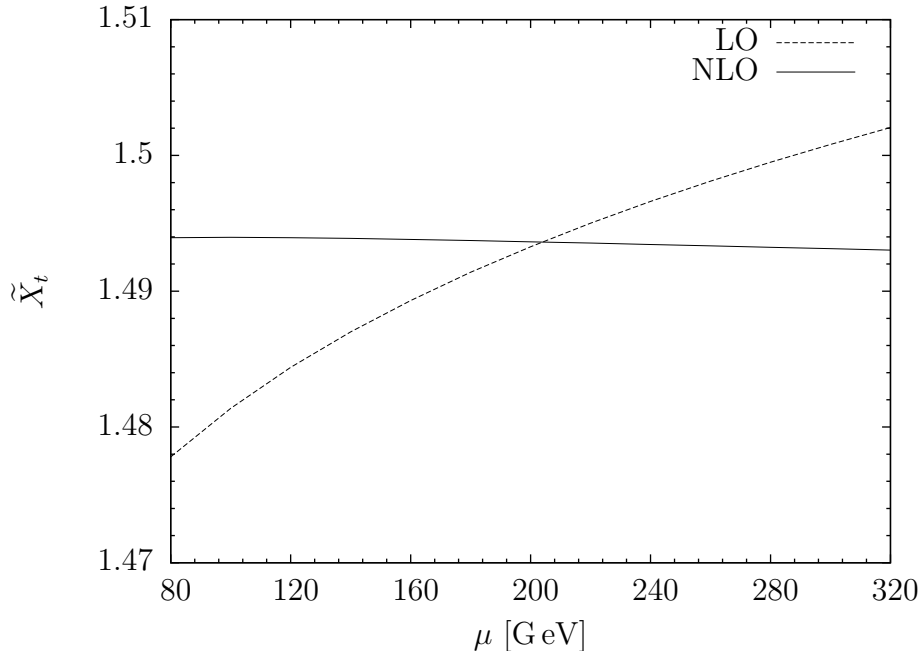


Figure 3:  $\tilde{X}_t$  (see text) as a function of  $\mu$ , for  $M_H = 155$  GeV. The LO result is represented by the dashed line, the solid line includes the full two-loop electroweak corrections, which cancel the  $\mu_t$ -dependence of the LO result almost completely.

We thus conclude that the on-shell definition of the masses together with the  $\overline{\text{MS}}$  definition of  $\sin^2 \theta_W$  is the best choice of the renormalisation scheme. We can read off the maximal difference of the three renormalisation schemes from the two NLO curves in Figure 5, right panel – it amounts to 0.27%. For our numerics below, we will take the average of the two curves and assign an error of  $\pm 0.134\%$  to  $X_t$ , as resulting from the remaining uncertainty of the electroweak correction. In total, using the central values from Table 1, we have

$$X_t = 1.469 \pm 0.017 \pm 0.002, \quad (4.2)$$

where the first error quantifies the remaining scale uncertainty of the QCD corrections, and the second error corresponds to the uncertainty of the electroweak corrections. Here and below, we determine the QCD error on  $X_t$  by varying the scale  $\mu_c$  between 80 GeV and 320 GeV. Accordingly, our central value of  $X_t$  is the average of  $\max_{\mu} X_t(\mu)$  and  $\min_{\mu} X_t(\mu)$ , where  $\mu \in [60 \text{ GeV}, 320 \text{ GeV}]$ .

Next, let us comment on the validity of the large- $m_t$  expansion of the full result, which can be gleaned from Figure 5: It is now evident that it is always a bad approximation to the full result, as has actually been expected before [9, 29].

For convenience we provide an approximate, yet very accurate formula for the NLO

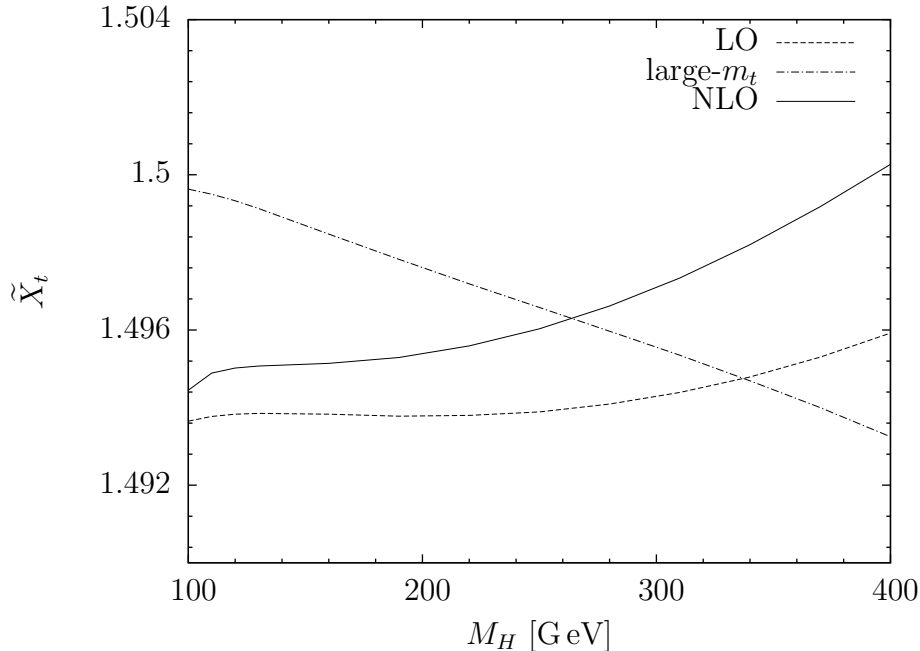


Figure 4:  $\tilde{X}_t$  as a function of  $M_H$ . The LO result is represented by the dashed line, the solid line shows the result including the full two-loop electroweak corrections. The NLO corrections in the limit of large top-quark mass are represented by the dashed-dotted line.

electroweak correction factor  $r_X = 1 + X_t^{(EW)}/X_t^{(0)}$ :

$$r_X = 1 - A + B \cdot C^{(M_t/165 \text{ GeV})} - D \left( \frac{M_t}{165 \text{ GeV}} \right) \quad (4.3)$$

where

$$A = 1.11508, \quad B = 1.12316, \quad C = 1.15338, \quad D = 0.179454. \quad (4.4)$$

It approximates the full result within the limits  $160 \text{ GeV} \leq M_t \leq 170 \text{ GeV}$  to an accuracy of better than  $\pm 0.05\%$ .

Finally, we update the theoretical prediction of the branching ratios, including the effect of the full two-loop electroweak corrections. After summation over the three neutrino flavours the resulting branching ratio for  $K^+ \rightarrow \pi^+ \nu \bar{\nu}$  can be written as<sup>2</sup> [1, 2, 30]

$$\begin{aligned} \text{Br}(K^+ \rightarrow \pi^+ \nu \bar{\nu}(\gamma)) \\ = \kappa_+(1 + \Delta_{\text{EM}}) \left[ \left( \frac{\text{Im}\lambda_t}{\lambda^5} X_t \right)^2 + \left( \frac{\text{Re}\lambda_c}{\lambda} (P_c + \delta P_{c,u}) + \frac{\text{Re}\lambda_t}{\lambda^5} X_t \right)^2 \right]. \end{aligned} \quad (4.5)$$

<sup>2</sup>We have omitted a term which arises from the implicit sum over lepton flavours in  $P_c$  because it amounts to only 0.2% of the branching ratio.

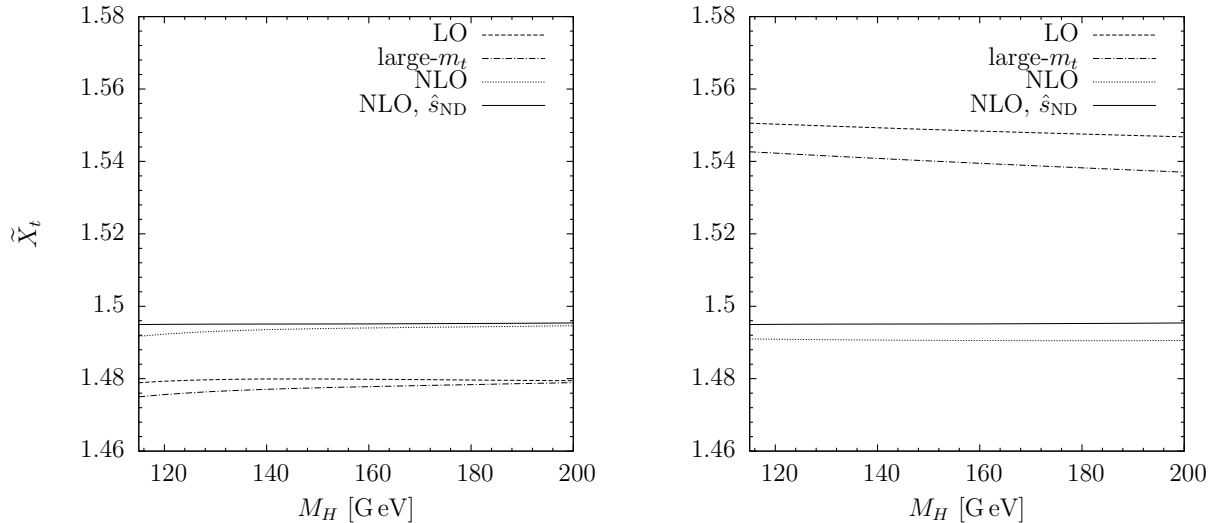


Figure 5:  $\tilde{X}_t$  as a function of  $M_H$ , in two different renormalisation schemes. The dashed lines show the LO results, the dashed-dotted lines the LO results including the electroweak corrections in the large- $m_t$  limit. The full two-loop results are represented by the dotted lines. The left panel shows the results where all parameters are defined in the  $\overline{\text{MS}}$  scheme. By contrast, in the right panel, all parameters apart from  $\alpha$  are defined in the on-shell scheme. For comparison, we also plot in both panels the NLO result, where all masses are defined on-shell and all couplings in the  $\overline{\text{MS}}$  scheme. It is represented by the solid lines.

The parameter

$$P_c(X) = \frac{1}{\lambda^4} \left( \frac{2}{3} X^e + \frac{1}{3} X^\tau \right) \quad (4.6)$$

describes the short-distance contribution of the charm quark, where  $\lambda = |V_{us}|$ , and has been calculated including electroweak corrections, in Reference [6]. The charm quark contribution of dimension-eight operators at the charm quark scale  $\mu_c$  [31] combined with long distance contributions were calculated in Reference [30] to be

$$\delta P_{c,u} = 0.04 \pm 0.02. \quad (4.7)$$

The hadronic matrix element of the low-energy effective Hamiltonian can be extracted from the well-measured  $K_{l3}$  decays, including isospin breaking and long-distance QED radiative corrections [27, 32, 33]. The long-distance contributions are contained in the parameters  $\kappa_+$ , including NLO and partially NNLO corrections in chiral perturbation theory.  $\Delta_{\text{EM}}$  denotes the long distance QED corrections [27].

Including the two-loop electroweak corrections to  $X_t$ , we find for the branching ratio of the charged mode

$$\text{Br}(K^+ \rightarrow \pi^+ \nu \bar{\nu}) = (7.81_{-0.71}^{+0.80} \pm 0.29) \times 10^{-11}, \quad (4.8)$$

The first error is related to the uncertainties in the input parameters. The main contributions are ( $V_{cb} : 56\%$ ,  $\bar{\rho} : 21\%$ ,  $m_c : 8\%$ ,  $m_t : 6\%$ ,  $\bar{\eta} : 4\%$ ,  $\alpha_s : 3\%$ ,  $\sin^2 \theta_W : 1\%$ ). The second error quantifies the remaining theoretical uncertainty. In detail, the contributions are ( $\delta P_{c,u} : 46\%$ ,  $X_t(\text{QCD}) : 24\%$ ,  $P_c : 20\%$ ,  $\kappa_+ : 7\%$ ,  $X_t(\text{EW}) : 3\%$ ), respectively.

The branching ratio of the  $CP$ -violating neutral mode involves the top-quark contribution only and can be written as

$$\text{Br}(K_L \rightarrow \pi^0 \nu \bar{\nu}) = \kappa_L \left( \frac{\text{Im} \lambda_t}{\lambda^5} X_t \right)^2. \quad (4.9)$$

Again, the hadronic matrix element can be extracted from the  $K_{l3}$  decays and is now parametrised by  $\kappa_L$  [27]. There are no more long-distance contributions, which makes this decay channel exceptionally clean.

Whereas the  $CP$ -conserving contribution to the branching ratio is completely negligible compared to the direct  $CP$ -violating contribution within the Standard Model [34], the indirect  $CP$ -violating contribution is of the order of 1% and should be included at the current level of accuracy. This can be achieved by multiplying the branching ratio with the factor [35]

$$1 - \sqrt{2} |\epsilon_K| \frac{1 + P_c(X)/(A^2 X_t) - \rho}{\eta}, \quad (4.10)$$

where  $A = V_{cb}/\lambda^2$ , and  $\epsilon_K$  describes indirect  $CP$  violation in the neutral Kaon system. Taking this factor into account, and including again the full two-loop electroweak corrections, we find

$$\text{Br}(K_L \rightarrow \pi^0 \nu \bar{\nu}) = (2.43_{-0.37}^{+0.40} \pm 0.06) \times 10^{-11}. \quad (4.11)$$

The first error is again related to the uncertainties in the input parameters. Here main contributions are ( $V_{cb} : 54\%$ ,  $\bar{\eta} : 39\%$ ,  $m_t : 6\%$ ). The contributions to the second, theoretical uncertainty are ( $X_t(\text{QCD}) : 73\%$ ,  $\kappa_L : 18\%$ ,  $X_t(\text{EW}) : 8\%$ ,  $\delta P_{c,u} : 1\%$ ), respectively. All errors have been added in quadrature.

## 5 Conclusions

In this paper, we have calculated the complete two-loop electroweak matching corrections to  $X_t$ , the top-quark contribution to the rare decays  $K_L \rightarrow \pi^0 \nu \bar{\nu}$ ,  $K^+ \rightarrow \pi^+ \nu \bar{\nu}$ , and  $B \rightarrow X_{d,s} \nu \bar{\nu}$ . This is in particular important for rare kaon decays: future proposals aim at an experimental accuracy of 3% for the branching ratios, while the leading order electroweak scheme ambiguity is of similar size. Our calculation reduces the scheme ambiguity in  $X_t$  from  $\pm 2\%$  to  $\pm 0.134\%$ . The resulting theory uncertainty in the branching ratios is rendered from dominant to negligible.

The absolute corrections are small in a renormalisation scheme where on-shell masses and  $\overline{\text{MS}}$  coupling constants are used for the electroweak sector. In addition, we analyse

the convergence in the  $\overline{\text{MS}}$  scheme and the on-shell scheme to estimate the remaining perturbative uncertainty.

Our analytic results are summarised by an approximate, but very accurate formula. We also give the leading term in a small  $\sin\theta_W$  expansion. The full expression can be obtained upon request from the authors.

## Acknowledgements

We would like to thank Gerhard Buchalla, Andrzej Buras, and Paolo Gambino for useful discussions and comments.

## A $\sin\theta_W$ Expansion

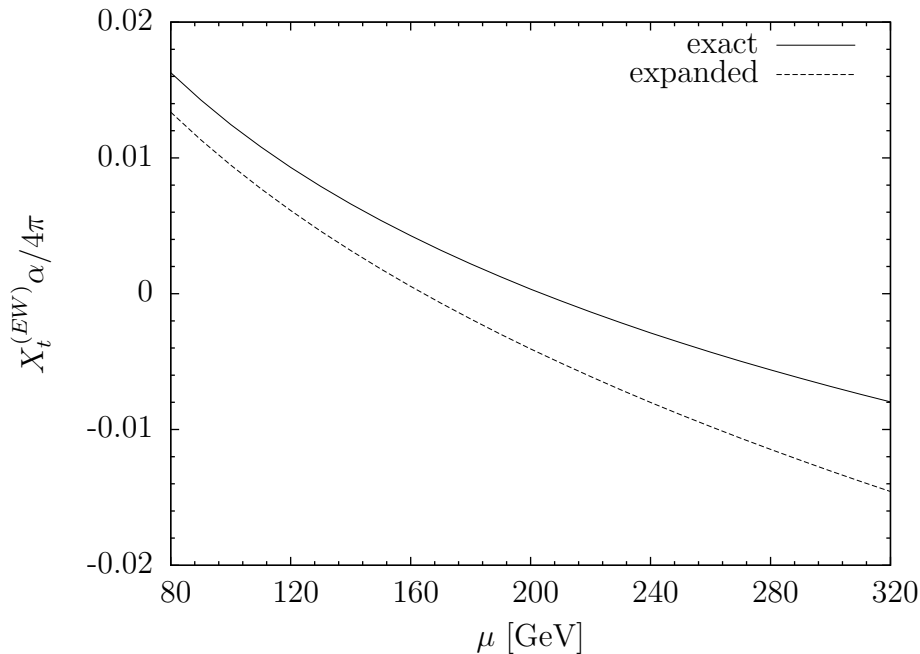


Figure 6: The  $\sin\theta_W$  expansion of  $X_t^{(EW)}\alpha/4\pi$  in the  $\overline{\text{MS}}$  scheme as a function of the renormalisation scale  $\mu$ . The solid line shows the full result, while the dashed line corresponds to the leading term of the expansion.

The explicit expression of the full two-loop electroweak correction  $X_t^{(EW)}$  is too long to be given explicitly here. The result significantly simplifies if we expand in the small parameter  $\sin\theta_W$  - see Figure 6 for the validity of the expansion.

In the  $\overline{\text{MS}}$  scheme, after normalising the effective Hamiltonian to  $G_F$ , we find

$$X^{(EW)}(x_t, a, \hat{s}_{\text{ND}}, \mu) = \frac{1}{128\hat{s}_{\text{ND}}^2} \left( \sum_{i=1}^{17} c_i A_i + \mathcal{O}(\hat{s}_{\text{ND}}) \right), \quad (\text{A.1})$$

where  $a = (M_H/m_t^{\overline{\text{MS}}})^2$ ,

$$\begin{aligned} c_1 &= \frac{1}{3a(x_t - 1)^2 x_t}, & c_2 &= \frac{1}{(x_t - 1)^3 (ax_t - 1)} \varphi_1\left(\frac{1}{4}\right), \\ c_3 &= \frac{1}{2(x_t - 1)^3 (ax_t - 1)} \varphi_1\left(\frac{a}{4}\right), & c_4 &= \frac{1}{2(x_t - 1)^3 (ax_t - 1)} \varphi_1\left(\frac{1}{4x_t}\right), \\ c_5 &= \frac{1}{2(x_t - 1)^3 (ax_t - 1)} \varphi_1\left(\frac{x_t}{4}\right), & c_6 &= \frac{1}{(x_t - 1)^3 (ax_t - 1)} \varphi_1\left(\frac{ax_t}{4}\right), \\ c_7 &= \frac{1}{2a^2 x_t^2 (x_t - 1)^3 (ax_t - 1)} \varphi_2\left(\frac{1}{ax_t}, \frac{1}{a}\right), & c_8 &= \frac{1}{ax_t - 1} \log^2(a), \\ c_9 &= \frac{1}{3(x_t - 1)^3 (ax_t - 1)} \log(x_t), & c_{10} &= \frac{1}{2a(x_t - 1)^4 x_t (ax_t - 1)} \log^2(x_t), \\ c_{11} &= \frac{1}{(x_t - 1)^2} \log\left(\frac{\mu^2}{M_W^2}\right), & c_{12} &= \frac{1}{(x_t - 1)^3} \log(x_t) \log\left(\frac{\mu^2}{M_W^2}\right), \\ c_{13} &= \frac{1}{(x_t - 1)^2 (ax_t - 1)} \log(a), & c_{14} &= \frac{1}{2a(x_t - 1)^3 x_t (ax_t - 1)} \log(x_t) \log(a), \\ c_{15} &= \frac{1}{(x_t - 1)^2} \text{Li}_2(1 - a), & c_{16} &= \frac{1}{ax_t} \text{Li}_2(1 - x_t), \\ c_{17} &= \frac{1}{a(x_t - 1)^2 x_t} \text{Li}_2(1 - ax_t) \end{aligned}$$

and

$$\begin{aligned} A_1 &= + (16 - 48a)\pi^2 + (288a - (32 - 88a)\pi^2)x_t + (2003a + 4(4 - 6a - a^2)\pi^2)x_t^2 \\ &\quad + (9a(93 + 28a) - 4a(3 - 2a + 8a^2)\pi^2)x_t^3 \\ &\quad + (3a(172 - 49a - 32a^2) + 4a(20 - a + 16a^2)\pi^2)x_t^4 \\ &\quad - (3a(168 + 11a - 24a^2) + 4a(45 + 8a^2)\pi^2)x_t^5 \\ &\quad + 96a\pi^2 x_t^6, \end{aligned}$$

$$A_2 = -768x_t - (525 - 867a)x_t^2 + (303 + 318a)x_t^3 - 195ax_t^4,$$

$$\begin{aligned} A_3 &= -8(95 - 67a + 11a^2)x_t^2 + 2(662 - 78a - 177a^2 + 40a^3)x_t^3 \\ &\quad - (608 + 476a - 595a^2 + 114a^3)x_t^4 + (44 + 188a - 321a^2 + 103a^3 - 8a^4)x_t^5 \\ &\quad - a(28 - 72a + 33a^2 - 4a^3)x_t^6, \end{aligned}$$

$$\begin{aligned} A_4 &= +48 - 10(57 + 4a)x_t + 51(29 + 10a)x_t^2 - (841 + 1265a)x_t^3 + (308 + 347a)x_t^4 \\ &\quad - (28 - 40a)x_t^5 + 12ax_t^6, \end{aligned}$$

$$\begin{aligned}
A_5 &= + 768 + (816 - 768a)x_t + (1240 - 1232a)x_t^2 - 4(415 + 2a)x_t^3 + (311 + 722a)x_t^4 \\
&\quad + (145 - 267a)x_t^5 - (36 + 51a)x_t^6 + 20ax_t^7, \\
A_6 &= + 328x_t - (536 + 900a)x_t^2 + (208 + 1584a + 670a^2)x_t^3 - a(668 + 1161a + 225a^2)x_t^4 \\
&\quad + a^2(479 + 362a + 28a^2)x_t^5 - a^3(143 + 42a)x_t^6 + 16a^4x_t^7, \\
A_7 &= + 32 - 4(44 - 9a)x_t + (384 - 322a - 400a^2)x_t^2 - (400 - 869a - 1126a^2 - 696a^3)x_t^3 \\
&\quad + 2(80 - 488a - 517a^2 - 631a^3 - 264a^4)x_t^4 \\
&\quad + (48 + 394a + 269a^2 + 190a^3 + 882a^4 + 196a^5)x_t^5 \\
&\quad - (64 - 58a - 89a^2 - 95a^3 + 34a^4 + 296a^5 + 32a^6)x_t^6 \\
&\quad + (16 - 59a - 79a^2 + 256a^3 - 239a^4 + 57a^5 + 48a^6)x_t^7 + (1 - a)^3a^2(29 + 16a)x_t^8, \\
A_8 &= + 28a^2x_t^2 - 32a^3x_t^3, \\
A_9 &= - 288 + 36(1 + 8a)x_t + 6(647 + 87a)x_t^2 + 5(55 - 927a - 132a^2)x_t^3 \\
&\quad - (1233 + 98a - 879a^2 - 192a^3)x_t^4 + (360 + 1371a - 315a^2 - 264a^3)x_t^5 \\
&\quad - 24a(17 - 4a^2)x_t^6, \\
A_{10} &= + 32 + 4(-44 + 29a)x_t - 12(-32 + 77a + 31a^2)x_t^2 \\
&\quad + 2(-200 + 837a + 767a^2 + 182a^3)x_t^3 - 2(-80 + 625a + 905a^2 + 520a^3 + 82a^4)x_t^4 \\
&\quad + (48 + 1079a + 590a^2 + 1002a^3 + 462a^4 + 32a^5)x_t^5 \\
&\quad + (-64 - 1160a - 501a^2 - 364a^3 - 486a^4 - 72a^5)x_t^6 \\
&\quad + (16 + 729a + 1038a^2 + 38a^3 + 238a^4 + 52a^5)x_t^7 \\
&\quad - a(192 + 743a + 50a^3 + 12a^4)x_t^8 + 192a^2x_t^9, \\
A_{11} &= + 16x_t + 324x_t^2 - 36x_t^4, \\
A_{12} &= + 216x_t - 672x_t^2 + 152x_t^3, \\
A_{13} &= - 16x_t + (16 - 42a)x_t^2 + (16 + 21a + 60a^2)x_t^3 \\
&\quad - (16 - 21a + 45a^2 + 32a^3)x_t^4 - a^2(7 - 24a)x_t^5, \\
A_{14} &= - 32 + (144 - 68a)x_t + (-240 + 334a + 332a^2)x_t^2 + (160 - 551a - 660a^2 - 364a^3)x_t^3 \\
&\quad + a(329 + 451a + 650a^2 + 164a^3)x_t^4 + (-48 - a - 59a^2 - 523a^3 - 316a^4 - 32a^5)x_t^5 \\
&\quad + (16 - 43a - 93a^2 + 255a^3 + 287a^4 + 32a^5)x_t^6 - a^2(-29 + 42a + 103a^2 + 8a^3)x_t^7, \\
A_{15} &= - 144(1 - a)^2x_t^2 + 144(1 - a)^2x_t^3 - 36(1 - a)^2x_t^4, \\
A_{16} &= - 32 + 96a + (48 - 32a)x_t - 176ax_t^2 - (16 - 74a)x_t^3 + 212ax_t^4,
\end{aligned}$$

$$A_{17} = -32 + (64 - 100a)x_t - 8(4 - 34a - 29a^2)x_t^2 - 4a(34 + 170a + 33a^2)x_t^3 \\ + 8a^2(47 + 51a + 4a^2)x_t^4 - 16a^3(15 + 4a)x_t^5 + 32a^4x_t^6.$$

Here we use

$$\text{Li}_2(\xi) = - \int_0^1 \frac{\log(1 - \xi t)}{t} dt,$$

and the two-loop functions  $\varphi_1$  and  $\varphi_2$  are given by [17]

$$\varphi_1(z) = \begin{cases} 4\sqrt{\frac{z}{1-z}}\text{Cl}_2(2\arcsin(\sqrt{z})), & 0 \leq z < 1, \\ \frac{1}{\lambda_z} \left( 2\ln^2 \frac{1-\lambda_z}{2} - 4\text{Li}_2 \frac{1-\lambda_z}{2} - \ln^2(4z) + \frac{1}{3}\pi^2 \right), & z > 1, \end{cases} \quad (\text{A.2})$$

and

$$\varphi_2(x, y) = \begin{cases} \frac{1}{\lambda} \left\{ \frac{\pi^2}{3} + 2\ln\left(\frac{1}{2}(1+x-y-\lambda)\right)\ln\left(\frac{1}{2}(1-x+y-\lambda)\right) - \ln x \ln y \right. \\ \left. - 2\text{Li}_2\left(\frac{1}{2}(1+x-y-\lambda)\right) - 2\text{Li}_2\left(\frac{1}{2}(1-x+y-\lambda)\right) \right\}, & \lambda^2 \geq 0, \sqrt{x} + \sqrt{y} \leq 1, \\ \frac{2}{\sqrt{-\lambda^2}} \left\{ \text{Cl}_2\left(2\arccos\left(\frac{-1+x+y}{2\sqrt{xy}}\right)\right) + \text{Cl}_2\left(2\arccos\left(\frac{1+x-y}{2\sqrt{x}}\right)\right) \right. \\ \left. + \text{Cl}_2\left(2\arccos\left(\frac{1-x+y}{2\sqrt{y}}\right)\right) \right\}, & \lambda^2 \leq 0, \sqrt{x} + \sqrt{y} \geq 1. \end{cases} \quad (\text{A.3})$$

Here  $\lambda_z = \sqrt{1 - 1/z}$  and  $\lambda = \sqrt{(1-x-y)^2 - 4xy}$ . The Clausen function is defined by  $\text{Cl}_2(z) = -\int_0^\theta d\theta \ln|2\sin(\theta/2)|$ .

## B The large- $m_t$ Expansion

The two-loop electroweak corrections to the  $bbZ$  vertex, denoted by  $\tau_b^{(2)}$ , have been calculated in the limit of a large top-quark mass by Barbieri et al. in [36, 37] and were confirmed by Fleischer, Tarasov, and Jegerlehner [38], who found a particularly simple analytic form of the results. Buchalla and Buras have extracted from this result the corrections to the  $sdZ$  vertex, which they used for their analysis of the  $K \rightarrow \pi\nu\bar{\nu}$  decays in [9]. We will now take the limit  $m_t \rightarrow \infty$  in our complete result for the  $sd\nu\nu$  transition and compare it with the result in [38].

Several important points should be mentioned here: As observed in [9], only  $Z$  penguin diagrams contribute to the  $sd\nu\nu$  transition in the large- $m_t$  limit. The results in [38] have been obtained in the so-called ‘‘gaugeless limit’’, where in particular the  $W$  boson field does not appear. Accordingly, the parameter corresponding to our  $x_t$  is defined in [38] by  $x_t \equiv \sqrt{2}G_\mu m_t^2 / (16\pi^2)$  and will be denoted by  $\tilde{x}_t$  in our paper. As a consequence, the result

for  $\tau_b^{(2)}$  is normalised to  $G_F^2$  in [38]. On the other hand, we performed a full Standard Model calculation and afterwards took the limit  $m_t \rightarrow \infty$ .

Thus we now take the large- $m_t$  expansion of our result, factor out  $G_F^2$ , and perform a finite renormalisation of the top-quark mass in our LO result, by replacing  $m_t^{\overline{\text{MS}}} = M_t + \delta M_t$ , in order to transform into the on-shell scheme. Here  $\delta M_t$  is given in the large- $m_t$  limit by

$$\frac{\delta M_t}{M_t} = \frac{e^2}{16\pi^2 s_W^2} x_t \left( \frac{3}{a} + 1 - \frac{1}{2}a - \frac{1}{16}(4a^{1/2} - a^{3/2})g(a) + \frac{1}{16}a^2 \log a \right), \quad (\text{B.1})$$

and

$$g(a) = 2\sqrt{a-4} \left[ \operatorname{arctanh} \left( \frac{2-a}{\sqrt{(a-4)a}} \right) + \operatorname{arctanh} \left( \sqrt{\frac{a}{a-4}} \right) \right]. \quad (\text{B.2})$$

In this way we reproduce the result in [38]:

$$\begin{aligned} \tau_b^{(2),\text{on-shell}} &= 9 - \frac{13}{4}a - 2a^2 - \left( \frac{1}{24} + \frac{7}{12}a^2 - \frac{1}{2}a^3 \right) \pi^2 - \left( \frac{19}{4}a + \frac{3}{2}a^2 \right) \ln a \\ &\quad - \left( \frac{7}{4}a^2 - \frac{3}{2}a^3 \right) \ln^2 a - \left( \frac{7}{4} - \frac{15}{2}a + \frac{39}{4}a^2 - 4a^3 \right) \operatorname{Li}_2(1-a) - \left( 2 - \frac{a}{2} \right) \sqrt{a}g(a) \\ &\quad - \frac{1}{2} \left( 7 - 18a + \frac{33}{4}a^2 - a^3 \right) \varphi_1 \left( \frac{a}{4} \right). \end{aligned} \quad (\text{B.3})$$

It corresponds to the effective Hamiltonian in the limit of large top-quark mass

$$\mathcal{H}_{\text{eff}} = \frac{4G_F}{\sqrt{2}} \frac{\alpha}{2\pi \sin^2 \theta_W} \lambda_t \left( \frac{x_t}{8} + \frac{\alpha}{4\pi} \frac{x_t^2}{32 \sin^2 \theta_W} (3 + \tau_b^{(2)}) \right) Q_\nu. \quad (\text{B.4})$$

Our result in the  $\overline{\text{MS}}$  scheme is given by

$$\begin{aligned} \tau_b^{(2),\overline{\text{MS}}} &= -2 - \frac{11}{4}a - 2a^2 - \left( \frac{1}{24} + \frac{7}{12}a^2 - \frac{a^3}{2} \right) \pi^2 \\ &\quad - \left( \frac{7}{4}a + 2a^2 \right) \ln a - \left( \frac{7}{4}a^2 - \frac{3}{2}a^3 \right) \ln^2 a \\ &\quad - \left( \frac{7}{4} - \frac{15}{2}a + \frac{39}{4}a^2 - 4a^3 \right) \operatorname{Li}_2(1-a) - \frac{1}{2} \left( 7 - 18a + \frac{33}{4}a^2 - a^3 \right) \varphi_1 \left( \frac{a}{4} \right) \end{aligned} \quad (\text{B.5})$$

for  $\mu_t = M_t$ . It is normalised to  $G_F$  and thus independent of the tadpole contribution.

## References

- [1] G. Buchalla and A. J. Buras. “The rare decays  $K^+ \rightarrow \pi^+ \nu \bar{\nu}$  and  $K_L \rightarrow \mu^+ \mu^-$  beyond leading logarithms”. Nucl. Phys. **B412**:106, 1994. doi:10.1016/0550-3213(94)90496-0. e-print:hep-ph/9308272.

- [2] G. Buchalla and A. J. Buras. “The rare decays  $K \rightarrow \pi\nu\bar{\nu}$ ,  $B \rightarrow X\nu\bar{\nu}$  and  $B \rightarrow l^+l^-$ : An update”. Nucl. Phys. **B548**:309, 1999. doi:10.1016/S0550-3213(99)00149-2. e-print:hep-ph/9901288.
- [3] M. Gorbahn and U. Haisch. “Effective Hamiltonian for non-leptonic  $|\Delta F| = 1$  decays at NNLO in QCD”. Nucl. Phys. **B713**:291, 2005. doi:10.1016/j.nuclphysb.2005.01.047. e-print:hep-ph/0411071.
- [4] A. J. Buras, M. Gorbahn, U. Haisch and U. Nierste. “The rare decay  $K^+ \rightarrow \pi^+\nu\bar{\nu}$  at the next-to-next- to-leading order in QCD”. Phys. Rev. Lett. **95**:261805, 2005. doi:10.1103/PhysRevLett.95.261805. e-print:hep-ph/0508165.
- [5] A. J. Buras, M. Gorbahn, U. Haisch and U. Nierste. “Charm quark contribution to  $K^+ \rightarrow \pi^+\nu\bar{\nu}$  at next-to-next-to-leading order”. JHEP **11**:002, 2006. e-print:hep-ph/0603079.
- [6] J. Brod and M. Gorbahn. “Electroweak Corrections to the Charm Quark Contribution to  $K^+ \rightarrow \pi^+\nu\bar{\nu}$ ”. Phys. Rev. **D78**:034006, 2008. doi:10.1103/PhysRevD.78.034006. e-print:0805.4119.
- [7] G. Buchalla and A. J. Buras. “QCD corrections to the  $\bar{s}dZ$  vertex for arbitrary top quark mass”. Nucl. Phys. **B398**:285, 1993. doi:10.1016/0550-3213(93)90110-B.
- [8] M. Misiak and J. Urban. “QCD corrections to FCNC decays mediated by Z-penguins and W-boxes”. Phys. Lett. **B451**:161, 1999. doi:10.1016/S0370-2693(99)00150-1. e-print:hep-ph/9901278.
- [9] G. Buchalla and A. J. Buras. “Two-loop large- $m_t$  electroweak corrections to  $K \rightarrow \pi\nu\bar{\nu}$  for arbitrary Higgs boson mass”. Phys. Rev. **D57**:216, 1998. doi:10.1103/PhysRevD.57.216. e-print:hep-ph/9707243.
- [10] T. Inami and C. S. Lim. “Effects of Superheavy Quarks and Leptons in Low-Energy Weak Processes  $K_L \rightarrow \mu\bar{\mu}$ ,  $K^+ \rightarrow \pi^+\nu\bar{\nu}$  and  $K^0 \leftrightarrow \bar{K}^0$ ”. Prog. Theor. Phys. **65**:297, 1981 [Erratum-ibid. **65**:1772, 1981]. doi:10.1143/PTP.65.297.
- [11] W. J. Marciano and A. Sirlin. “Electroweak Radiative Corrections to  $\tau$  Decay”. Phys. Rev. Lett. **61**:1815, 1988. doi:10.1103/PhysRevLett.61.1815.
- [12] T. van Ritbergen and R. G. Stuart. “On the precise determination of the Fermi coupling constant from the muon lifetime”. Nucl. Phys. **B564**:343, 2000. doi:10.1016/S0550-3213(99)00572-6. e-print:hep-ph/9904240.
- [13] F. Jegerlehner, M. Y. Kalmykov and O. Veretin. “ $\overline{\text{MS}}$  vs. pole masses of gauge bosons: Electroweak bosonic two-loop corrections”. Nucl. Phys. **B641**:285, 2002. doi:10.1016/S0550-3213(02)00613-2. e-print:hep-ph/0105304.

- [14] F. Jegerlehner, M. Y. Kalmykov and O. Veretin. “ $\overline{\text{MS}}$  vs pole masses of gauge bosons. II: Two-loop electroweak fermion corrections”. Nucl. Phys. **B658**:49, 2003. doi:10.1016/S0550-3213(03)00177-9. e-print:hep-ph/0212319.
- [15] G. Degrandi, P. Gambino and A. Sirlin. “Precise calculation of  $M_W$ ,  $\sin^2 \theta^{\overline{\text{MS}}}$ , and  $\sin^2 \theta_{\text{eff}}$ ”. Phys. Lett. **B394**:188, 1997. doi:10.1016/S0370-2693(96)01677-2. e-print:hep-ph/9611363.
- [16] C. Bobeth, M. Misiak and J. Urban. “Photonic penguins at two loops and  $m_t$ -dependence of  $\text{BR}(B \rightarrow X_s l^+ l^-)$ ”. Nucl. Phys. **B574**:291, 2000. doi:10.1016/S0550-3213(00)00007-9. e-print:hep-ph/9910220.
- [17] A. I. Davydychev and J. B. Tausk. “Two loop selfenergy diagrams with different masses and the momentum expansion”. Nucl. Phys. **B397**:123, 1993. doi:10.1016/0550-3213(93)90338-P.
- [18] T. Hahn. “Generating Feynman diagrams and amplitudes with FeynArts 3”. Comput. Phys. Commun. **140**:418, 2001. doi:10.1016/S0010-4655(01)00290-9. e-print:hep-ph/0012260.
- [19] J. A. M. Vermaseren. “New features of FORM” 2000. e-print:math-ph/0010025.
- [20] T. L. Trueman. “Spurious anomalies in dimensional renormalization”. Z. Phys. **C69**:525, 1996. doi:10.1007/s002880050057. e-print:hep-ph/9504315.
- [21] M. Awramik, M. Czakon, A. Freitas and G. Weiglein. “Precise prediction for the W-boson mass in the standard model”. Phys. Rev. **D69**:053006, 2004. doi:10.1103/PhysRevD.69.053006. e-print:hep-ph/0311148.
- [22] K. G. Chetyrkin, J. H. Kuhn and M. Steinhauser. “RunDec: A Mathematica package for running and decoupling of the strong coupling and quark masses”. Comput. Phys. Commun. **133**:43, 2000. doi:10.1016/S0010-4655(00)00155-7. e-print:hep-ph/0004189.
- [23] K. Nakamura. “Review of particle physics”. J. Phys. **G37**:075021, 2010. doi:10.1088/0954-3899/37/7A/075021.
- [24] Tevatron Electroweak Working Group. “Combination of CDF and D0 Results on the Mass of the Top Quark” 2010. e-print:1007.3178.
- [25] K. G. Chetyrkin *et al.* “Charm and Bottom Quark Masses: an Update”. Phys. Rev. **D80**:074010, 2009. doi:10.1103/PhysRevD.80.074010. e-print:0907.2110.
- [26] M. Antonelli *et al.* “Precision tests of the Standard Model with leptonic and semileptonic kaon decays” 2008. e-print:0801.1817.
- [27] F. Mescia and C. Smith. “Improved estimates of rare K decay matrix-elements from  $K_{\ell 3}$  decays”. Phys. Rev. **D76**:034017, 2007. doi:10.1103/PhysRevD.76.034017. e-print:0705.2025.

- [28] J. Charles *et al.* “CP violation and the CKM matrix: Assessing the impact of the asymmetric  $B$  factories”. *Eur. Phys. J.* **C41**:1, 2005. doi:10.1140/epjc/s2005-02169-1. e-print:hep-ph/0406184.
- [29] P. Gambino, A. Kwiatkowski and N. Pott. “Electroweak effects in the  $B^0 - \overline{B}^0$  mixing”. *Nucl. Phys.* **B544**:532, 1999. doi:10.1016/S0550-3213(98)00860-8. e-print:hep-ph/9810400.
- [30] G. Isidori, F. Mescia and C. Smith. “Light-quark loops in  $K \rightarrow \pi\nu\bar{\nu}$ ”. *Nucl. Phys.* **B718**:319, 2005. doi:10.1016/j.nuclphysb.2005.04.008. e-print:hep-ph/0503107.
- [31] A. F. Falk, A. Lewandowski and A. A. Petrov. “Effects from the charm scale in  $K^+ \rightarrow \pi^+\nu\bar{\nu}$ ”. *Phys. Lett.* **B505**:107, 2001. doi:10.1016/S0370-2693(01)00343-4. e-print:hep-ph/0012099.
- [32] W. J. Marciano and Z. Parsa. “Rare kaon decays with ‘missing energy’”. *Phys. Rev.* **D53**:1, 1996. doi:10.1103/PhysRevD.53.R1.
- [33] J. Bijnens and K. Ghorbani. “Isospin breaking in  $K\pi$  vector form-factors for the weak and rare decays  $K_{\ell 3}$ ,  $K \rightarrow \pi\nu\bar{\nu}$  and  $K \rightarrow \pi\ell^+\ell^-$ ” 2007. e-print:0711.0148.
- [34] G. Buchalla and G. Isidori. “The CP conserving contribution to  $K_L \rightarrow \pi^0\nu\bar{\nu}$  in the standard model”. *Phys. Lett.* **B440**:170, 1998. doi:10.1016/S0370-2693(98)01088-0. e-print:hep-ph/9806501.
- [35] G. Buchalla and A. J. Buras. “ $K \rightarrow \pi\nu\bar{\nu}$  and high precision determinations of the CKM matrix”. *Phys. Rev.* **D54**:6782, 1996. doi:10.1103/PhysRevD.54.6782. e-print:hep-ph/9607447.
- [36] R. Barbieri, M. Beccaria, P. Ciafaloni, G. Curci and A. Vicere. “Two loop heavy top effects in the Standard Model”. *Nucl. Phys.* **B409**:105, 1993. doi:10.1016/0550-3213(93)90448-X.
- [37] R. Barbieri, M. Beccaria, P. Ciafaloni, G. Curci and A. Vicere. “Radiative correction effects of a very heavy top”. *Phys. Lett.* **B288**:95, 1992. doi:10.1016/0370-2693(92)91960-H. e-print:hep-ph/9205238.
- [38] J. Fleischer, O. V. Tarasov and F. Jegerlehner. “Two loop large top mass corrections to electroweak parameters: Analytic results valid for arbitrary Higgs mass”. *Phys. Rev.* **D51**:3820, 1995. doi:10.1103/PhysRevD.51.3820.